

See discussions, stats, and author profiles for this publication at: <https://www.researchgate.net/publication/231674538>

# Tapping Mode Atomic Force Microscopy Investigation of Poly(amidoamine) Core–Shell Tecto(dendrimers) Using Carbon Nanoprobes

ARTICLE *in* LANGMUIR · MARCH 2002

Impact Factor: 4.46 · DOI: 10.1021/la025538s

---

CITATIONS

43

---

READS

21

8 AUTHORS, INCLUDING:



**Bradford G Orr**

University of Michigan

172 PUBLICATIONS 7,049 CITATIONS

SEE PROFILE



**James R Baker**

University of Michigan

423 PUBLICATIONS 18,831 CITATIONS

SEE PROFILE

# Tapping Mode Atomic Force Microscopy Investigation of Poly(amidoamine) Core–Shell Tecto(dendrimers) Using Carbon Nanoprobes

Theodore A. Betley, Jessica A. Hessler, Almut Mecke, Mark M. Banaszak Holl,\*  
Bradford G. Orr,\* Srinivas Uppuluri, Donald A. Tomalia, and  
James R. Baker, Jr.

Departments of Chemistry and Physics and the Center for Biologic Nanotechnology,  
University of Michigan, Ann Arbor, Michigan 48109

Received January 15, 2002

Carbon nanoprobes were utilized in tapping mode atomic force microscopy investigations to highlight the topographic differences between poly(amidoamine) (PAMAM) dendrimers, two-dimensional arrays of PAMAM dendrimers, and PAMAM core–shell tecto(dendrimers). The PAMAM core–shell tecto(dendrimers) used for this study consist of a shell of generation five (G5) dendrimers covalently linked to a G7 core. The volumes measured for the PAMAM core–shell tecto(dendrimers) suggest a 75–100% saturation of shell G5 dendrimers about the G7 core. This compares favorably with theoretical predictions that 12 G5 dendrimers should pack to form a shell about a G7 core. The effect of different imaging substrates was also explored. Tecto(dendrimers) imaged on hydrophobic surfaces experience a 6-fold increase in maximum peak height and a 3-fold decrease in diameter as compared to those imaged on mica. Measured volume is invariant.

## Introduction

The recent discovery of super- and supramolecular dendrimer structures by Percec et al.,<sup>1,2</sup> Tomalia et al.,<sup>3–5</sup> and Schlüter et al.<sup>6</sup> elegantly illustrates the combination of self-assembly with rational synthesis. In recent reports from the Tomalia laboratories, individual poly(amidoamine) (PAMAM) dendrimers, synthesized using the original divergent synthesis method, form the basic building blocks of the structure.<sup>7</sup> A supermolecular core–shell tecto(dendrimer) is then self-assembled by placing a larger dendrimer core in a vast excess of the small dendrimers. The solution assembly of the large and small dendrimers is similar to the classic problem of packing spheres. For a given pair of diameters, one can predict the ideal number of dendrimers that will assemble about the central core.<sup>8</sup> After self-assembly has taken place, a cross-linking agent is added to covalently link the assembled dendrimers together. For example, a generation seven (G7) dendrimer could be used as the core surrounded by G5 dendrimers. A schematic two-dimensional cross section of such a core–shell tecto(dendrimer) is illustrated in Figure 1.

In this paper, we explore two important questions regarding the PAMAM core–shell tecto(dendrimers). First, can one obtain direct topographic evidence that demonstrates this core–shell structure is different from

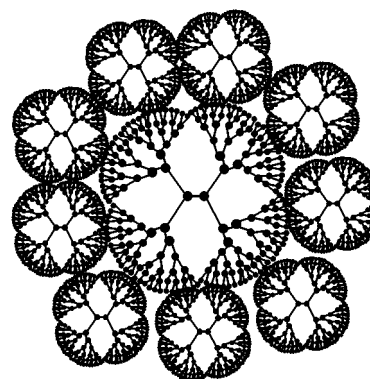


**Figure 1.** Schematic representation of PAMAM core–shell tecto(dendrimer).

that of a normal PAMAM dendrimer or a noncovalent cluster of dendrimers? The resolution obtained in topographic studies published to date make both the single dendrimers and the core–shell tecto(dendrimers) appear as spherical caps, albeit with significantly different volumes.<sup>3</sup> Second, can one count the number of smaller dendrimers linked around the core? The ability to make such measurements is important for characterizing such supermolecular species and for directing future synthetic approaches.

To address these questions, we have imaged a G7(G5)<sub>n</sub> PAMAM dendrimer sample using an atomic force microscope (AFM) equipped with carbon nanoprobes. The unique core–shell tecto(dendrimer) topography is compared and contrasted with that of the single dendrimers and dendrimer clusters formed by noncovalent interactions. In addition, volumes measured for the core–shell tecto(dendrimers) have been correlated with specific numbers of shell G5 dendrimers surrounding the G7 core.

## Experimental Section

**Materials.** Ethylenediamine (EDA) core poly(amidoamine) dendrimers and PAMAM core–shell tecto(dendrimers) were obtained as methanol or aqueous solutions from The University

- (1) Percec, V.; Cho, W.-D.; Mosier, P. E.; Ungar, G.; Yeardley, D. J. *J. Am. Chem. Soc.* **1998**, *120*, 11061–11070.
- (2) Percec, V.; Ahn, C.-H.; Ungar, G.; Yeardley, D. J. P.; Möller, M.; Sheiko, S. S. *Nature* **1998**, *391*, 161–164.
- (3) Li, J.; Swanson, D. R.; Qin, D.; Brothers, H. M.; Peihler, L. T.; Tomalia, D.; Meier, D. J. *Langmuir* **1999**, *15*, 7347–7350.
- (4) Uppuluri, S.; Swanson, D. R.; Spindler, R.; Tomalia, D. A. *Polym. Mater. Sci. Eng.* **1999**, *80*, 55.
- (5) Uppuluri, S.; Swanson, D. R.; Piehler, L. T.; Li, J.; Hagnauer, G. L.; Tomalia, D. A. *Adv. Mater.* **2000**, *12*, 796–800.
- (6) Karakaya, B.; Claussen, W.; Gessler, K.; Saenger, W.; Schlüter, A.-D. *J. Am. Chem. Soc.* **1997**, *119*, 3296–3301.
- (7) Dvornic, P. R.; Tomalia, D. A. *Poly(amidoamine) dendrimers*; Oxford University Press: Oxford, 1999.
- (8) Mansfield, M. L.; Rakesh, L.; Tomalia, D. A. *J. Chem. Phys.* **1996**, *105*, 3245–3249.

of Michigan's Center for Biologic Nanotechnology. The core-shell tecto(dendrimers) were synthesized using procedures previously described.<sup>4,5</sup> The solutions were typically diluted to 1 nM concentrations with deionized, distilled, Millipore (0.1  $\mu\text{m}$ ) filtered water and stored at  $-4^\circ\text{C}$  until use.

**Substrate Preparation.** Three substrates were used for this study. Fresh mica substrates were prepared by cleaving the mica surface prior to sample deposition. Trimethylsilane-terminated silica substrates ( $\text{SiO}_2\text{-TMS}$ ) were prepared by rinsing pieces of Si(111) wafers with ethanol followed by soaking the wafer in chlorotrimethylsilane for 20 min and drying under flowing air prior to sample deposition. Thin films of hydridosilsesquioxane (HSQ) resins (also known as FOx resin) were prepared by spin-coating the HSQ resin dissolved in methylisobutyl ketone (60  $\text{mg}/\text{cm}^3$ ) onto a freshly cleaved mica surface. The thin polymer films were spin-coated at 1300 rpm for 45 s. HSQ resin was obtained from Dow Corning and used without further purification.

**Sample Preparation.** Sample solutions of dendrimers (typically 1–5 nM in concentration with pH of either  $\sim 6$  or  $\sim 1$ ) were spin-coated on substrates at 100–200 rpm in air for 5 min. Aqueous dendrimer solutions were acidified to pH  $\sim 1$  by dropwise addition of concentrated hydrochloric acid (12.6 M). Sample pH was verified via litmus paper.

**AFM Measurements.** All measurements were made using tapping mode operation with a Nanoscope IIIa multimode scanning probe microscope from Digital Instruments (Santa Barbara, CA) using a "J" vertical engage scanner. Tapping mode etched silicon probes (TESP; spring constant,  $k_0$ , 40–71 N/m and force constant,  $f_0$ , 351–422 kHz) and carbon nanoprobees were used for imaging. Knowledge of tip shape is crucial for making accurate volume measurements.<sup>9,10</sup> To achieve this goal, carbon nanoprobees were grown on force etched silicon probes (FESP;  $k_0 = 1.7\text{--}2.9\text{ N/m}$ ,  $f_0 = 70\text{--}83\text{ kHz}$ ) using literature procedures.<sup>11–13</sup> Radius of curvature for both commercial TESP and carbon nanoprobees was measured using Nioprobe standards available from GeneralMicro.<sup>14,15</sup> The carbon nanoprobe tips used for this study were measured prior to obtaining dendrimer images and had a radius of curvature of  $2.6 \pm 0.2\text{ nm}$ , consistent with the literature.<sup>13</sup> Representative TESP tips were measured and determined to have radii of 3.9 and 4.2 nm, consistent with manufacturer specifications. Tip convolution was determined by subtracting the tip geometry contribution from cross-sectional line scans. For the purposes of the calculations, tip geometry was assumed to be spherical with diameters as reported in the literature (carbon nanoprobees  $d_{\text{tip}} = 2.5\text{ nm}$ ; TESP probes  $d_{\text{tip}} = 4\text{ nm}$  from manufacturer specifications).<sup>13</sup> The purpose for determining the tip convolution was to estimate volume increases to AFM images as a function of aspect ratios.<sup>16</sup> Identical results were obtained for the G9 dendrimers from both kinds of tips. Differences in volume measurement from tip convolution induced by variation between the carbon nanoprobees ( $d_{\text{tip}} = 2.6 \pm 0.2\text{ nm}$ ) were significantly less than the systematic error obtained for multiple images of the same tecto(dendrimer) using the same tip.

**Calculations.** Densities of PAMAM dendrimers have been reported for generations 0–5.<sup>17</sup> To estimate the densities of later generations, the published densities were fit to a saturation model in the form of

$$\text{density (g}/\text{cm}^3) = a - be^{(-cn)}$$

where  $a$ ,  $b$ , and  $c$  are empirical parameters and  $n$  is the generation number. The values for the parameters are  $a = 1.232$ ,  $b = 0.05540$ ,

and  $c = 0.4741$ . The volumes for the samples in the AFM images were determined via numerical integration of the data using the instrument software. The largest pixel size used for determining sample volume was  $3 \times 3\text{ \AA}$ .

## Results and Discussion

**The Topography of PAMAM G7(G5)<sub>n</sub> Core-Shell Tecto(dendrimers).** Topographic differences between single PAMAM dendrimers, two-dimensional arrays of PAMAM dendrimers, and PAMAM core-shell tecto(dendrimers) were examined using carbon-nanoprobe modified FESP tips to obtain the highest possible resolution. The bonding of the G5 shell dendrimers about the G7 core is not understood in detail. Shell coordination is achieved by self-assembly followed by the addition of covalent linking agents. Neither the exact number of shell dendrimers attached to the core nor the number of covalent links between shell dendrimer and core is known.<sup>4,5</sup> An idealized picture of a core-shell tecto(dendrimer) can be envisioned by considering a rigid spherical core surrounded by a close-packed shell of rigid, spherical smaller generation dendrimers (Figure 1).<sup>8</sup> However, substantial evidence indicates that PAMAM dendrimers tend to spread over supporting substrates when significant surface interactions can take place.<sup>16,18–21</sup> An example of this is illustrated in Figure 2a for a single PAMAM G9 dendrimer. Although the theoretical spherical diameter of the G9 dendrimer is 10.7 nm, the dendrimer imaged on mica has a diameter of 31 nm and a height of 4.1 nm.<sup>16</sup> Core-shell tecto(dendrimers) have also been observed to spread over mica surfaces.<sup>3</sup> Previous AFM studies using conventional Si tips obtained clear images of individual tecto(dendrimers) but were not able to resolve any internal structure.

AFM images obtained using carbon nanotube modified FESP tips highlight the differences between single PAMAM dendrimers, two-dimensional arrays of PAMAM dendrimers, and the PAMAM core-shell tecto(dendrimers) (Figure 2). An image of single, ninth generation (G9) PAMAM dendrimers deposited onto mica from a solution of pH = 1 is provided in panel a. The isolated dendrimers extend over approximately 30 nm and stand 4 nm in height. Panel b illustrates two heptameric noncovalently linked clusters of single G9 dendrimers on mica. For these G9 dendrimers arranged in two-dimensional close-packed clusters, the measured dendrimer heights increase to 5–7 nm with a concomitant decrease in the observed diameters to  $\sim 15\text{ nm}$  (panel e). Panel c shows a single G7(G5)<sub>n</sub> tecto(dendrimer) on a mica substrate. The tecto(dendrimer) spreads over 46 nm in diameter yet has a maximum peak height of just 1.6 nm (panel f). The tecto(dendrimer) lacks the rigidity of the G9 single dendrimers and arrays. Multiple inflection points are readily apparent in the line scan as compared to the smooth curve observed for a single dendrimer. Unlike the two-dimensional cluster of single dendrimers, individual dendrimers are not readily apparent in the topographic image. Overall, on comparison of panels a–c, the tecto(dendrimers) are easily distin-

(9) Hansma, H. G.; Ho, J. H. *Annu. Rev. Biophys. Biomol. Struct.* **1994**, *23*, 115–139.

(10) Shao, Z.; Mou, J.; Czajkowsky, D. M.; Yang, J.; Yuan, J.-Y. *Adv. Phys.* **1996**, *45*, 1–86.

(11) Cheung, C. L.; Hafner, J. H.; Odom, T. W.; Kim, K.; Lieber, C. M. *Appl. Phys. Lett.* **2000**, *76*, 3136–3138.

(12) Hafner, J. H.; Cheung, C. L.; Lieber, C. M. *Nature* **1999**, *398*, 761–762.

(13) Hafner, J. H.; Cheung, C. L.; Lieber, C. M. *J. Am. Chem. Soc.* **1999**, *121*, 9750–9751.

(14) Westra, K. L.; Thomson, D. J. *J. Vac. Sci. Technol., B* **1994**, *12*, 3176–3181.

(15) Westra, K. L.; Mitchell, A. W.; Thomson, D. J. *J. Appl. Phys.* **1993**, *74*, 3608–3610.

(16) Betley, T. A.; Banaszak Holl, M. M.; Orr, B.; Swanson, D. R.; Tomalia, D. A.; Baker, J. R. *Langmuir* **2001**, *17*, 2768–2773.

(17) Uppuluri, S.; Keinath, S. E.; Tomalia, D. A.; Dvornic, P. R. *Macromolecules* **1998**, *31*, 4498–4510.

(18) Hierlemann, A.; Campbell, J. K.; Baker, L. A.; Crooks, R. M.; Ricco, A. J. *J. Am. Chem. Soc.* **1998**, *120*, 5323–5324.

(19) Tokuhisa, H.; Zhao, M.; Baker, L. A.; Phan, V. T.; Dermody, D. L.; Garcia, M. E.; Peez, R. F.; Crooks, R. M.; Mayer, T. M. *J. Am. Chem. Soc.* **1998**, *120*, 4492–4501.

(20) Tsukruk, V. V.; Rinderspacher, R.; Bliznyuk, V. N. *Langmuir* **1997**, *13*, 2171–2176.

(21) Li, J.; Peihler, L. T.; Qin, D.; Baker, J. R.; Tomalia, D.; Meier, D. *Langmuir* **2000**, *16*, 5613–5616.



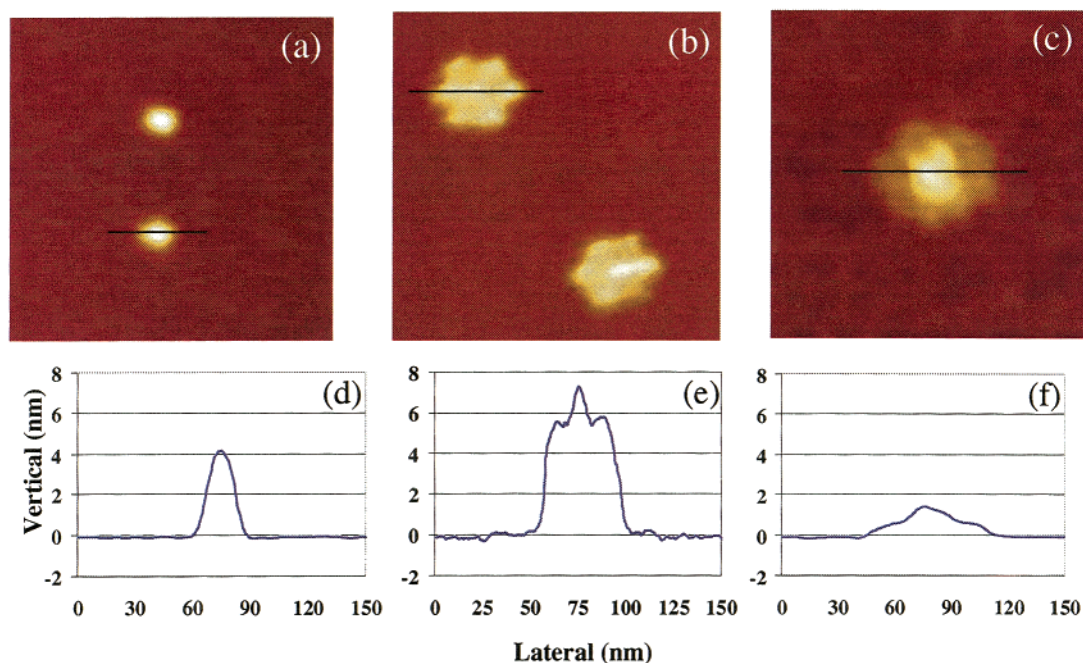


**Figure 2.** (a) AFM image of single G9 dendrimers deposited on mica from a buffer solution of pH = 1, scanned with a carbon nanoprobe ( $150 \times 150$  nm, vertical scale = 15 nm). The highlighted dendrimer dimensions are diameter = 31 nm, height = 4.1 nm, and volume =  $778 \text{ nm}^3$ . (b) AFM image of G9 dendrimers clustered on mica in a close-packed arrangement from a buffer solution of pH = 1, scanned with a carbon nanoprobe ( $150 \times 150$  nm, vertical scale = 15 nm). The highlighted dendrimer cluster has a volume of  $5580 \text{ nm}^3$  (seven G9 dendrimers). (c) AFM image of a single G7(G5)<sub>n</sub> tecto(dendrimer) deposited on mica from a neutral, aqueous solution ( $150 \times 150$  nm, vertical scale = 3 nm). The tecto(dendrimer) dimensions are diameter = 51 nm (horizontal), height = 1.4 nm, and volume =  $940 \text{ nm}^3$ . Horizontal line scans (panels d–f) are provided for the highlighted dendrimers in images a–c. Important features to note include the increased dendrimer heights when in close-packed arrays and the very low aspect ratio of the tecto(dendrimer). Although the volumes of the structures in images a and c are similar, the more rigid G9 structure spreads over less of the mica substrate than the G7(G5)<sub>n</sub> tecto(dendrimer).

guishable from the single dendrimers by topographic information alone.

Additional comments regarding the observed diameter and height of the PAMAM tecto(dendrimer) on mica are in order. If it is assumed that dendrimers behave as rigid spheres, the sum of two G5 and one G7 diameter lead to a prediction of  $\sim 15$  nm for the diameter of the G7(G5)<sub>n</sub> tecto(dendrimer). Alternatively, an estimate of the expected diameter can be made by comparison to single dendrimers of similar molecular weight. For example, a G7(G5)<sub>12</sub> tecto(dendrimer) has a molecular weight of  $\sim 507\,000$ . A single PAMAM G9 dendrimer with a molecular weight of  $467\,000$  was experimentally determined to have a diameter of 36 nm and a height of 3.4 nm when deposited from a pH 6 solution onto mica.<sup>16</sup> On the basis of these observations, core-shell tecto(dendrimers) appear capable of greater elastic deformation than a single dendrimer of comparable molecular weight. These effects are highlighted by the line scans in Figure 2, panels d and f.

The comparisons highlighted in Figure 2 contrast the behavior of amine terminated PAMAM dendrimers (Figure 2a,b) with that of the tecto(dendrimer) which has a carboxylic acid terminated surface (Figure 2c). For this comparison to be valid, the amine and carboxylic acid terminated dendrimers must have similar deformation behavior on the mica substrate. To assess this, G9 PAMAM dendrimers terminated with carboxylic acid groups were deposited from a pH 1 solution and imaged on a mica substrate. Although these particles are nominally larger than the amine terminated dendrimers due to the addition of carboxylic acid groups on the surface, the change is small and a statistically significant difference was not obtained by AFM for the height, diameter, or volume. The images for the particles appear identical to those shown

in Figure 2a. In addition G7 PAMAM dendrimers terminated with carboxylic acid groups were deposited from a pH 1 solution and imaged on a mica substrate. Once again, no statistically significant difference in height, diameter, or volume was obtained as compared to that previously obtained for amine terminated dendrimers at pH 6 on mica.<sup>16</sup> We observed no difference in deformation behavior for amine and carboxylic acid terminated dendrimers on mica surfaces.

The measured diameters and heights are a sensitive function of the choice of imaging substrate. Our previous work demonstrated that for dendrimers deposited on HSQ resin films, the dendrimer-substrate interaction is limited to weak van der Waals interactions and the dendrimer spreading phenomena across the substrate is minimized.<sup>16</sup> Interaction between the dendrimer primary amine surface and the substrate likely causes this distortion of the molecular shape. The selection of a hydrophobic substrate for imaging drastically affects the observed dendrimer dimensions, presumably because fewer hydrogen bonds can be made. For cases where sample-substrate interaction is dominated solely by van der Waals interactions, the apparent height of the dendrimer samples increases with a concomitant decrease in the observed diameters.

Representative images of G7(G5)<sub>n</sub> on mica (panel a), SiO<sub>2</sub>-TMS (panel b), and HSQ resin substrates (panel c) are illustrated in Figure 3. Panel d compares line scans from cross-sectional analysis for the dendrimer on the three substrates. The maximum height of a single G7(G5)<sub>n</sub> dendrimer increases from 1.1 nm on mica, to 2.4 nm on SiO<sub>2</sub>-TMS, to 6.8 nm on HSQ resin. A related decrease in dendrimer diameter is also apparent. Measured diameters are 42, 29, and 14 nm for mica, SiO<sub>2</sub>-TMS, and HSQ resin, respectively. As a function of substrate, the PAMAM G7(G5)<sub>n</sub> tecto(dendrimer) adopts a maximum

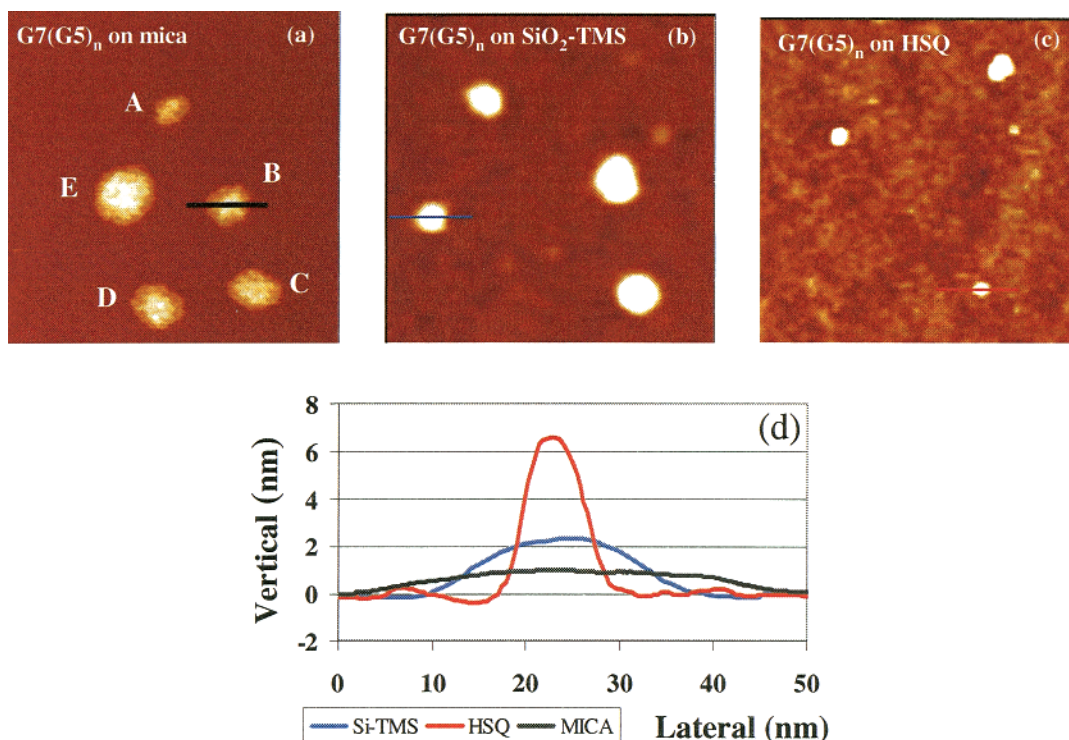


**Figure 3.** AFM images of G7(G5)<sub>n</sub> tecto(dendrimers) deposited from pH = 6 aqueous solutions (500 × 500 nm): (a) mica substrate, vertical scale = 3 nm; (b) SiO<sub>2</sub>-TMS substrate, vertical scale = 15 nm; (c) HSQ resin substrate, vertical scale = 25 nm. (d) Representative line scans of single tecto(dendrimers) as highlighted in panels a–c. The line scans are single measurements, not averaged line scans.

height between 7% (mica) and 45% (HSQ) of the theoretical diameter as predicted by rigid spheres. This is in contrast to single amine-capped G9 dendrimers that vary between 42% (mica) and 98% (HSQ) of the theoretical rigid sphere diameter.<sup>16</sup> Despite the considerable change in maximum height and lateral diameter, the dendrimers on mica, SiO<sub>2</sub>-TMS, and HSQ have consistent overall volumes. The single tecto(dendrimers) used for the line scans compared in Figure 3d have volumes of  $832 \pm 49 \text{ nm}^3$  (mica),  $810 \pm 48 \text{ nm}^3$  (SiO<sub>2</sub>-TMS), and  $842 \pm 51 \text{ nm}^3$  (HSQ). The line scans shown are single measurements representative of the sample average. These data add further support to the notion that the tecto(dendrimers) are capable of greater elastic deformation than single dendrimers of similar molecular weight.

Tecto(dendrimers) readily aggregate, even on mica substrates. Similar to the G9 dendrimers, the tecto(dendrimers) frequently form aggregates as opposed to singly binding to SiO<sub>2</sub>-TMS and HSQ substrates. As shown in Figure 3, tecto(dendrimer) aggregates do not form two-dimensional clusters on mica with individually resolvable features as single G9 dendrimers do. On both SiO<sub>2</sub>-TMS and HSQ, the tecto(dendrimers) formed pillar-like aggregates. These pillars, with diameters of ~50–80 nm and heights of 20–25 nm, were estimated to contain as many as 35 individual dendrimers. Finding large areas covered mainly by single tecto(dendrimers) is very difficult. Similar aggregation behavior of PAMAM G9 dendrimers on SiO<sub>2</sub>-TMS and HSQ has been previously observed.<sup>16</sup>

Choice of substrate also plays an interesting role in the imaged topography of the core–shell tecto(dendrimers). The less interacting substrates, SiO<sub>2</sub>-TMS and HSQ, give images with no discernible internal topographic features. However, a distinct topography is observed when the samples are imaged on mica. This change in imaging may arise because the tecto(dendrimers) are becoming more spherical with smaller topographic features when on the more hydrophobic surfaces. It is also possible that as the

tecto(dendrimers) become more spherical and have less contact with the surface, they can undergo elastic deformation during the imaging process effectively averaging out any discernible topographic features.

**Volume Analysis, Shell Filling, and Distribution of Dendrimers.** We have previously shown that differences between individual single PAMAM dendrimers within a given sample can be analyzed by AFM.<sup>16</sup> In particular, measured volume discrepancies between dendrimers (exceeding the uncertainty of individual measurements) have been attributed to differences in the polymers themselves. The images of the individual tecto(dendrimers) have obvious topographic differences (Figures 2c, 3a, and 6). The average volume measured for this representative set of tecto(dendrimer) images is  $893 \pm 70 \text{ nm}^3$ . This standard deviation of ~8% is twice as large as the error obtained when measuring the volume of G9 dendrimers.<sup>16</sup> This error corresponds to approximately the volume for a single G5 dendrimer. These two observations lead us to further explore the use of volume measurements for analyzing the compositions of the G7-(G5)<sub>n</sub> tecto(dendrimers).

The uncertainty regarding the core–shell bonding geometry makes the best approach for theoretical volume predictions of core–shell tecto(dendrimers) unclear. However, the volumes of individual PAMAM dendrimers have already been well characterized by AFM.<sup>16</sup> Figure 4 provides the experimentally measured volumes of single PAMAM dendrimers for generations five to nine deposited from pH = 1 and pH = 6 solution. The theoretical volumes, based on known molecular weights and estimated densities, are provided for comparison. The measured volumes exceed the theoretical values due to partial protonation of the dendrimer's primary amine surface functionalities (pH = 6) or surface and internal amines (pH = 1). The data series representing dendrimers deposited from acidic solutions (pH = 1) are provided to emphasize the ability of the polymers to expand upon protonation.<sup>22,23</sup> To



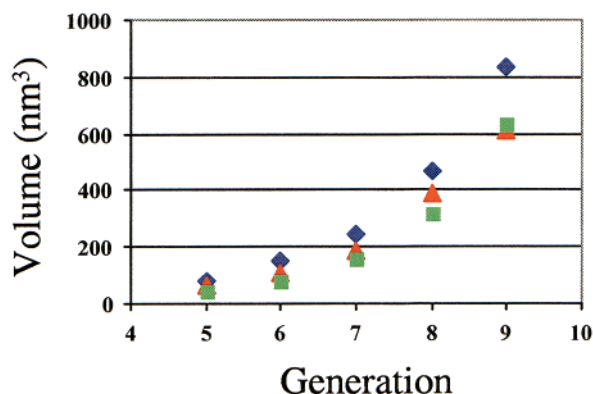


**Figure 4.** PAMAM dendrimer volumes as a function of generation. Dendrimer samples deposited on mica from solutions of pH = 1 (blue diamonds) and pH = 6 (red triangles). The green squares depict the theoretical volumes for generations five to nine based on known molecular weights and estimated densities.

estimate the volume of core-shell tecto(dendrimers), we will use the volumes for G5 and G7 single dendrimers deposited from solutions of pH = 6 as empirical benchmarks. In this fashion, we hope to roughly account for the observation that partial protonation effects give somewhat larger than expected volume measurements (by ~20%).<sup>16</sup> Recall that the volumes for amine terminated and carboxylic acid terminated G9 dendrimers were found to be identical within experimental error. Since the greatest difference in volume was anticipated for the G9 case, the use of the amine terminated G5 and G7 volumes appears reasonable.

The volumes for G5 and G7 dendrimers are  $62 \pm 3$  and  $187 \pm 10$  nm<sup>3</sup>, respectively (Figure 4).<sup>16</sup> Volume contributions from the linking molecule that covalently bonds the shell dendrimers to the core have been neglected. They should not contribute more than a few percent to the total volume and thus induce volume changes that are indiscernible by these AFM measurements. Simple summing of the G7 and G5 volumes yields estimated total volumes for G7(G5)<sub>n</sub> of 746, 808, 870, and 932 nm<sup>3</sup> for  $n = 9-12$ , respectively.

The single G7(G5)<sub>n</sub> tecto(dendrimers) featured in Figures 2, 3, and 6 have volumes ranging between 780 and 960 nm<sup>3</sup>. The tecto(dendrimer) in Figure 2c has a volume of  $940 \pm 56$  nm<sup>3</sup>. The tecto(dendrimers) labeled C and D in Figure 3 have volumes of  $958 \pm 57$  and  $928 \pm 56$  nm<sup>3</sup>, respectively. The measured volumes for these tecto(dendrimers) all fall within the range expected for a G7-(G5)<sub>12</sub> species ( $932 \pm \sim 60$  nm<sup>3</sup>). The tecto(dendrimers) used for the representative line scan analyses in Figure 3 have volumes consistent with G7(G5)<sub>10-11</sub>. Dendrimer B has a volume of  $832 \pm 49$  nm<sup>3</sup>, and the dendrimers used for line scans on SiO<sub>2</sub>-TMS and HSQ have volumes of  $810 \pm 48$  and  $842 \pm 51$  nm<sup>3</sup>, respectively. The tecto(dendrimer) labeled A in Figure 3 has a volume of  $782 \pm 47$  nm<sup>3</sup>, which is consistent with 9-10 G5 dendrimers surrounding the G7 core. The aggregate labeled E in Figure 3 has a volume of  $2440 \pm 146$  nm<sup>3</sup>, which could contain as many as three individual tecto(dendrimers).

Previous reports discussing the shell saturation for these core-shell tecto(dendrimers) have suggested 75-87% saturation levels are achieved. These values were deter-

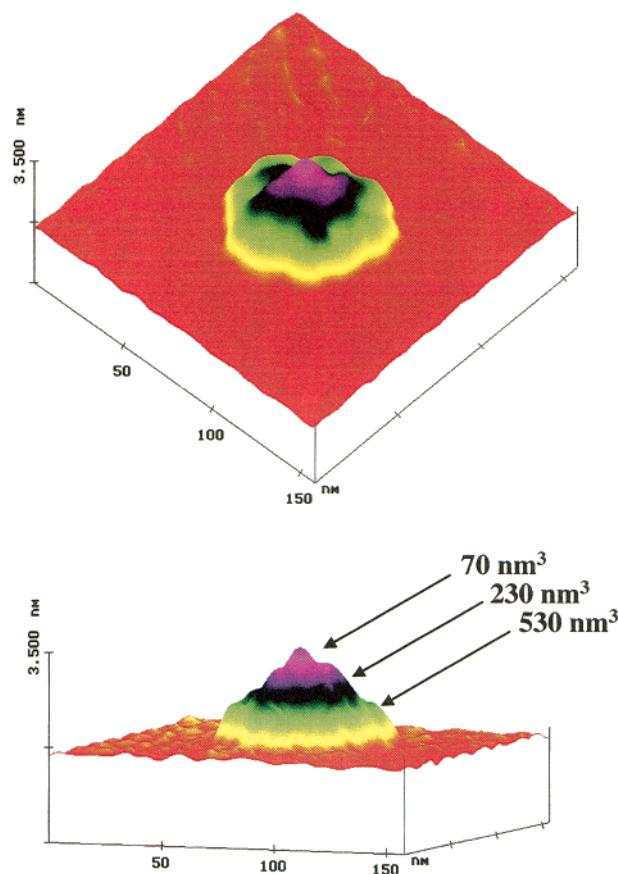


**Figure 5.** Three-dimensional view of core-shell PAMAM tecto(dendrimer) "B" from Figure 3a. This G7(G5)<sub>10-11</sub> sample was deposited on mica from a pH = 6 solution.

mined by consideration of matrix-assisted laser desorption ionization mass spectroscopy (MALDI-MS), polyacrylamide gel electrophoresis (PAGE), and AFM molecular weight determinations.<sup>3-5</sup> As we will discuss in the next section, the volumes provided by these AFM measurements were considerably larger than those reported here due to the estimation method used. However, these authors also assumed a density of 1 g/cm<sup>3</sup>, a considerably lower value than the known experimental studies of density indicate.<sup>17</sup> This set of assumptions led to an estimated molecular weight of 469 000 g/mol consistent with a G7(G5)<sub>10-11</sub> tecto(dendrimer).<sup>5</sup> MALDI-MS measurements yielded a molecular weight of 403 000 g/mol, consistent with G7(G5)<sub>9</sub>. PAGE yielded an estimate of 670 000 g/mol, consistent with G7(G5)<sub>17</sub>, a value for  $n$  that exceeds the theoretical packing limit of 12.<sup>5,8</sup>

The results presented in this paper find an average volume value of  $893 \pm 70$  nm<sup>3</sup>, consistent with G7(G5)<sub>11-12</sub>. Numerous perfectly saturated shells ( $n = 12$ ) and shells missing a single G5 ( $n = 11$ ) were imaged. Significantly less perfect shell filling,  $n = 9-10$ , has also occasionally been observed. The significant findings of this paper with respect to the measured volumes are 2-fold. First, using the identical sample employed by Uppuluri et al.,<sup>5</sup> we find numerous examples of perfect shell filling. We also observe a somewhat higher average filling with most of the tecto(dendrimers) imaged falling between  $n = 11$  and 12.

A three-dimensional, banded color image of tecto(dendrimer) B from Figure 3a is illustrated in Figure 5. The total measured volume is  $832 \pm 49$  nm<sup>3</sup>, consistent with G7(G5)<sub>10-11</sub>. The view also helps to highlight the three-dimensional asymmetry present for an individual

(22) van Duijvenbode, R. C.; Borkovec, M.; Koper, G. J. M. *Polymer* **1998**, *39*, 2657-2664.

(23) Koper, G. J. M.; van Genderen, M. H. P.; Elissen-Román, C.; Baars, M. W. P. L.; Meijer, E. W.; Borkovec, M. *J. Am. Chem. Soc.* **1997**, *119*, 66512-6521.

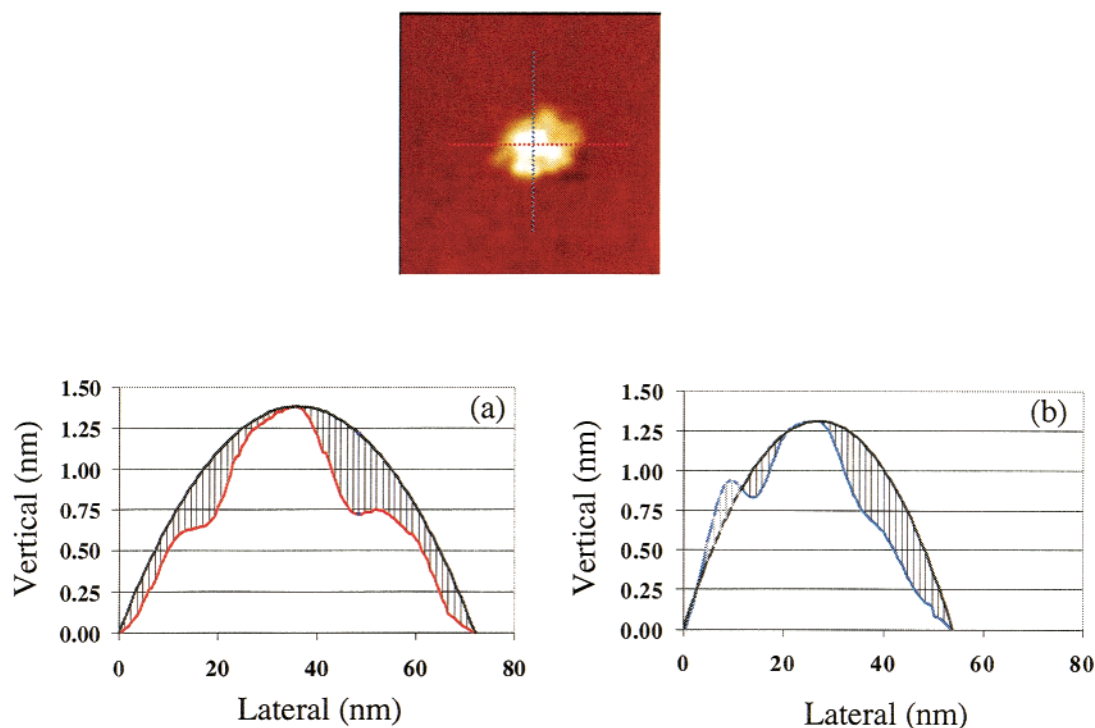


**Figure 6.** A single  $G7(G5)_n$  tectodendrimer on mica deposited from a neutral, aqueous solution ( $150 \times 150$  nm, vertical scale = 3 nm). (a) Representative horizontal line scan (red line) and the cross section from the spherical cap assumption (black line). The spherical cap estimation yields a volume of  $2826 \text{ nm}^3$ , 307% of the integrated volume of  $920 \text{ nm}^3$ . The shaded area between the series highlights the excess volume when the cap is convoluted into three dimensions. (b) Representative vertical line scan for the dendrimer (blue line) and the cross section from the spherical cap assumption (black line). The spherical cap estimation yields a volume of  $1505 \text{ nm}^3$ , 164% of the integrated volume. The asymmetry of the dendrimer is apparent in both the AFM height image and upon comparing the horizontal and vertical line scans (a) and (b).

tecto(dendrimer). This image is also useful for breaking down the overall structure into individual volume components. The pink asperity at the top of the image has a volume of  $\sim 70 \text{ nm}^3$ , about 10% larger than the anticipated volume of a G5 dendrimer. The purple region,  $\sim 230 \text{ nm}^3$ , is somewhat larger than expected for three G5 dendrimers. However, based on the schematic model shown in Figure 1, this region should consist of G5 and G7 dendrimers. The base of the structure, shown in green and yellow, has a volume of  $\sim 530 \text{ nm}^3$ , considerably larger than a single G7 ( $187 \text{ nm}^3$ ). The volume of this region is consistent with ca. six to seven G5 dendrimers and one G7 dendrimer.

Overall, the volume data presented are consistent with the schematic model of the tecto(dendrimer) structure presented in Figure 1. On the basis of this structural assumption, and empirically derived volumes for individual dendrimers, one finds good agreement in terms of the ranges of measured volume. The volumes are also readily explained in terms of numbers of G5 shell dendrimers present. Given that the structural hypothesis is correct and that the G5 and G7 components used in this synthesis have a low polydispersity, the AFM techniques described in this paper provide a powerful method for analyzing the degree and distribution of shell filling for this important general class of supermolecular materials. However, we must make clear that AFM volume measurements of this type do not provide an absolute method for structural determination. If the key core-shell structural hypothesis breaks down, the interpretations could become far more complicated and much less exact. For example, if a measured particle consisted of two G7 dendrimers and eight to nine G5 dendrimers, a volume of  $\sim 870\text{--}930 \text{ nm}^3$  is predicted. This volume range is consistent with that measured for all single tecto(dendrimer) images presented in this paper. Given the

significant elasticity noted in this work, a  $(G7)_2(G5)_{8-9}$  dendrimer cluster may not be distinguishable from a  $G7(G5)_{10-12}$  core-shell tecto(dendrimer). In the absence of independently characterized molecules of this type, absolute structure determination is impossible.

**Methods for Volume Analysis.** Previous workers estimated the volumes of the molecules using a spherical cap model.<sup>3,5</sup> Our previous work demonstrated the insufficiency of this estimation to accurately depict the volumes of single PAMAM dendrimers.<sup>16</sup> The AFM images of the tecto(dendrimers) presented in this work (Figures 2, 3, and 6) highlight the asymmetries present in the individual tecto(dendrimers). These asymmetries have not previously been reported as conventional AFM tips do not resolve these features.<sup>5</sup> The carbon-nanoprobe modified FESP tips were required to obtain this degree of resolution. In light of the distinct asymmetries measured, we thought it prudent to examine the spherical cap assumption in more detail.

The volumes of the individual molecules and clusters were determined via numerical integration of the data (i.e., the bearing method provided in the instrumental software). We have found the spherical cap assumption typically overestimates the true feature volume by a factor of 1.5–3 for the core-shell tecto(dendrimers). Figure 6 illustrates a single tecto(dendrimer) deposited on mica with horizontal and vertical line scans and the corresponding cross section of the spherical cap used to estimate the molecular volume. The shaded area between the sample line scan and spherical cap cross section becomes excess volume when convoluted into three dimensions. The volume yielded by the spherical cap model for the line scan in Figure 6a (horizontal) is  $2826 \text{ nm}^3$ , 307% of the integrated volume of  $920 \text{ nm}^3$ . The volume yielded by the line scan in Figure 6b (vertical) is  $1505 \text{ nm}^3$ , 164% of the

integrated volume. Note that depending on the line scan chosen to represent the volume of the tecto(dendrimer), a factor of  $\sim 2$  difference can be obtained in the volume due to the significant asymmetry of the individual core-shell tecto(dendrimer). The numerically integrated sample volume is unaffected by the molecular asymmetries and is a much more accurate and reliable measure of dendrimer volume.

### Conclusions

By use of carbon nanoprobe modified FESP tips, the AFM experiments presented here show the dramatic difference between single dendrimers, two-dimensional arrays of single dendrimers, and the as-synthesized supermolecular core-shell tecto(dendrimers). Comparing the observed tecto(dendrimer) volumes with empirically derived volume estimates allows the number of G5 shell dendrimers to be estimated. Numerous G7(G5)<sub>12</sub> species were imaged indicating the self-assembly method developed by Tomalia et al. is a highly effective method for

generating a covalently linked core-shell topology.<sup>5</sup> AFM experiments also highlight the effects of substrate upon the observed height, diameter, and volume of soft, deformable tecto(dendrimers). On a sufficiently hydrophobic surface such as HSQ resin, the tecto(dendrimers) are no longer imaged as flat disklike structures. Rather, they exhibit substantial height increases with concomitant diameter decreases.

**Acknowledgment.** This project has been funded with federal funds from the National Cancer Institute, National Institutes of Health, under Contract NOI-CO-97111. M.M.B.H. thanks the Alfred P. Sloan foundation for a research fellowship (1999–2002). H. Hansma and J. Li are thanked for fruitful discussions of this work. C. M. Lieber and his laboratory are thanked for providing a critical hands-on introduction to carbon-nanoprobe techniques.

LA025538S